Synthesize and Characterization of Styrene-*N*-Phenyl Maleimide/Montmorillonite Nanocomposites Prepared through Emulsion Polymerization

Guodong Liu, Liucheng Zhang, Zongjian Li, Xiongwei Qu

Institute of Polymer Science and Engineering, School of Chemical Engineering, Hebei University of Technology, Tianjin 300130, People's Republic of China

Received 8 June 2004; accepted 20 January 2005
DOI 10.1002/app.22211
Published online in Wiley InterScience (www.interscience.wiley.com).

ABSTRACT: Composites of organomodified (OMMT) and pristine montmorillonite (MMT) intercalated by styrene-*N*-phenyl maleimide (PMI) copolymer were prepared by emulsion intercalative polymerization. X-ray diffraction (XRD) and transmission electron microscopy results show that the dispersability of clay in the matrix was greatly improved by the incorporation of polar moiety PMI. The dispersability of OMMT in the matrix is better than MMT. XRD patterns of the extracted nanocomposites showed that d_{001} of the clay are much larger than that of the original OMMT and MMT, which indicates that the interaction of copolymer with the clay layers was greatly improved by incorporation with polar monomer PMI. The thermal property of the composites was greatly improved by the intercalation with clay. The DSC results showed that the glass transition of the composites became inconspicuous, which indicated that the movement of the polymer segment was extremely confined by the clay layer. The consistency factor of the melts of the composites increased monotonically with a decreasing flow index showing stronger shear thinning property of the composites. The rheological activity energy of the composites decreased more than that of the pure copolymer. © 2005 Wiley Periodicals, Inc. J Appl Polym Sci 98: 1010–1015, 2005

Key words: clay; emulsion polymerization; nanocomposites; *N*-phenyl maleimide; polystyrene

INTRODUCTION

Polymer/layered silicate nanocomposites (PLSN) have attracted considerable technological and scientific interest in recent years, especially after Nylon-6/montmorillonite nanocomposite was reported by Okada et al. in 1987.[1] This technological interest has stemmed from the dramatic enhancements in physical, thermal, and mechanical properties of PLSN materials with a minimal increase in density as a result of low inorganic loading.

The crystal structure of montmorillonite consists of two-dimensional layers formed by fusing two silica tetrahedral sheets to an edge-shared octahedral sheet of aluminum hydroxide. Stacking of the layers by weak dipolar or van der Waals forces leads to interlayers of galleries between the layers. The galleries are normally occupied by cations, which balance the charge deficiency that is generated by isomorphous substitution within the layers.

The most promising strategy for synthesizing polymer/clay nanocomposites is intercalation of polymer in layered hosts. In most cases, the synthesis involves either intercalation polymerization[2,3] or polymer intercalation from solution or melts.[4–6] However, the lack of affinity between the hydrophilic silicate interlayer and the hydrophobic organic monomers or polymers makes the synthetic situation difficult. This has led to approaches so far known to use organically modified silicates or suitable compatibilizers. Organically modified silicates are produced by a cation-exchange reaction between the silicate and an alkylammonium salt, which will improve the affinity between the clay and monomers or polymers.

The incorporation with Na^+ and/or Ca^{2+} enhances the hydrophilic property of the montmorillonite (MMT), which in turn leads to easy penetration and a high degree of water swelling. At the same time, an emulsion system consisting of an aqueous medium can contribute to the affinity between the hydrophilic host and the hydrophobic guest by the action of the emulsifier. Recently, polymer/montmorillonite nanacomposites prepared by emulsion polymerization have been developed by Lee and other researchers.[7–10]

Meanwhile, many studies showed that incorporation of polar moieties into the chain of the nonpolar polymer will greatly improve the dispersability of the clay in the polymer matrix.[11] Kawasumi and coworkers described the incorporation of end group modified oligomeric polypropylene to prepare PP/MMT nano-

Correspondence to: L. Zhang (gdliu@263.net).
Contract grant sponsor: National Science Foundation of Hebei Province; contract grant number: 202018.

© 2005 Wiley Periodicals, Inc.

composites.[12] For the preparation of PP/clay, PS/clay, and other nonpolar polymer/clay nanocompsites, maleic anhydride (MA)-grafted polymer was most widely used.[12–14] It was believed that the improvement is due to the strong hydrogen bonding between the polar functional group of MA and the oxygen group of silicates. *N*-Phenyl maleimide (PMI) has a structure similar to MA; it may also help the dispersability of the clay in polymer matrix and the intercalation of polymer chains into the gallery of the silicates. Meanwhile, the incorporation of the moiety of PMI can also improve the thermal property of the polymer greatly.[15] It is necessary to investigate the synergism of PMI and clay on the properties of the formed nanocomposites.

EXPERIMENTAL

Materials

Na-montmorillonite used in this paper was supplied by Huate Co. (Zhejiang Province, China). The clay was purified by dispersion of this crude clay into deionized water and separation of the noncolloidal impurities. The "solution" of clay was directly used in the preparation of polymer/MMT nanocomposites. The organomodified montmorillonite (OMMT) was obtained by cation exchange of the clay with cetyltrimethylammonium bromide as described in a previous paper.[16]

Styrene (Tianjin Chem Co., Tianjin, China) was of analytical purity and made free of inhibitor by washing with an aqueous solution of sodium hydroxide and then with deionized water, drying, and distilling under reduced pressure. PMI was supplied by Lanchou Chem Co. (Gansu Province, China) and recrystallized twice in a water/ethanol mixture (volume ratio 2 : 1).

Emulsion polymerization

A measured amount of montmorillonite suspension was added into a four-neck flask fitted with mechanical stirrer, thermometer, condenser (with a dropping funnel), and a nitrogen conduct. Then deionized water was added to a sum volume of 400 mL. After sonication for 1 h at room temperature, 9 g sodium lauryl sulfate (SLS) was added with gentle stirring. The temperature was then raised to 85°C and the initiator, potassium persulfate (1.8 g), was introduced to the reactor. The stirring rate was then raised to give a vigorous mixture of the system and 120 g of styrene/PMI (wt ratio 80 : 20) was then dropped into the system slowly 10 min later under nitrogen atmosphere. When there was no monomer left in the dropping funnel, the content in the flask was poured into about 400 mL of aluminum sulfate solution (3 wt %). The coagulated products was filtered and washed several times with hot water. The products were then dried, washed with ethanol for 24 h, and dried under reduced pressure at 60°C.

The preparation of styrene (St)-PMI/OMMT nanocomposites was only little different from the procedure described above. First, a measured amount of OMMT powder, deionized water, and SLS was added into the flask and stirred vigorously for about 20 min. Then the system was sonicated for 1 h at room temperature and heated to 85°C and the former step was as described above.

Characterization and measurements

X-ray diffraction (XRD) patterns were recorded by monitoring the diffraction angle 2θ from 1 to 30° on a DMAX-RC X-ray crystallographic unit. The unit was equipped with a Ni-filtered CuKα radiation ($\lambda = 0.154$ nm) source at a voltage of 50 kV and a current of 180 mA. The scanning speed and step size are 1°/min and 0.02°, respectively.

The morphological aspects of the composites have been examined by using transmission electron microscopy (TEM) to determine the internal micromorphology. A Hitachi H-800 TEM with an acceleration voltage of 80 kV was used.

Part of the pulverized product was extracted with hot chloroform for 5 days by means of Soxhlet extraction. The content of the intercalated or bonded macromolecules was determined gravimetrically. The nongrafted fraction of the copolymer was removed by continuous extraction and recovered by pouring the filtrate into a large amount of ethanol. Inherent viscosity of the recovered polymer was measured using an Ubbelohde viscometer and 1.0 g/dL chloroform solution at 25°C.

Thermogravimetric analysis (TGA) measurement were carried out by employing a DuPont TA-2000 component thermogravimetry (SDT 2960) instrument. The samples were heated to 600°C at a heating rate of 10°C/min under nitrogen atmosphere. The thermal properties of the composites were also measured by differential scanning calorimetry (DSC) using a DSC-2910 component of DuPont TA-2000 system. Samples of 10-mg mass were heated under nitrogen atmosphere to 200°C at a heating rate of 20°C/min. The data obtained from the second scan were accepted.

The rheological property of the composites was measured by a KLY-II flow tester ($L/d = 40$) at 200°C at different shearing stresses. The shear rate, $\dot{\gamma}'_w$, was improved for non-Newtonian.

RESULTS AND DISCUSSION

Structure characterization

It is difficult for nonpolar macromolecules to intercalate into the silicate layers, since the interaction is

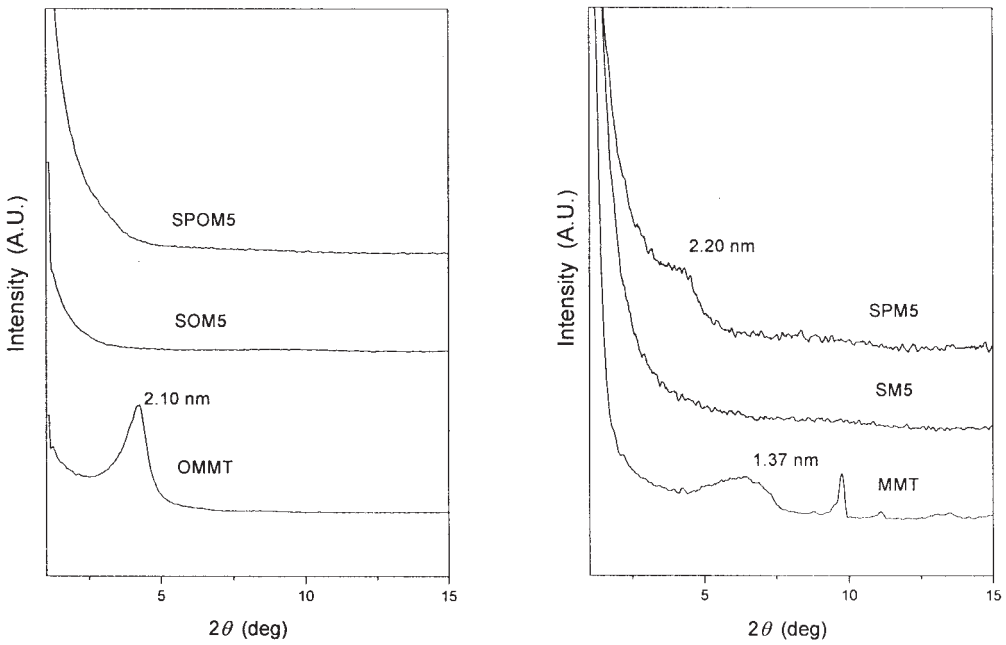

Figure 1 XRD patterns of OMMT, SOM5, SPOM5, MMT, SM5, and SPM5 composites.

thermodynamically unfavorable. So the incorporation of polar PMI moiety will enhance the intercalation between MMT and polymer due to the interaction between the alkylammonium salt or clay layer with maleimide groups.[17] It was also reported that maleic anhydride grafted polypropylene (PP-MA) can interact with layers of the clay through strong hydrogen bonding between the polar functional group and the oxygen group of the silicate.[18]

Figure 1 shows XRD profiles of OMMT, MMT, and St-PMI/montmorillonite (demonstrated with SPOM*x* or SPM*x* in the following text, where *x* represents the content of montmorillonite in the composites). The peaks correspond to the 001 reflections of the clay. The basal spacing of the OMMT increased from 1.37 nm for pristine MMT to 2.10 nm. After intercalative polymerization, the peak of montmorillonite disappears, except for the SPM5 composite, which shows a peak at d_{001} = 2.20 nm. It seems that the copolymer intercalates between the layers of MMT during polymerization and eventually expands or exfoliates the silicate layers.

Although XRD is the most efficient method to demonstrate the gallery change of the clay in composites, it is not enough to characterize the dispersability of the clay. TEM photographs of SOM5, SM5, SPOM5, and SPM5 are shown in Figure 2. In the case of SM5, the silicate layers were aggregated and only part of the layers has been delaminated. The dispersability of clay in the PS matrix is very poor; this is also why there are no diffraction peaks in its XRD patterns. While the dispersity of OMMT in PS is greatly improved, due to the intercalative agent it interacts with both the clay

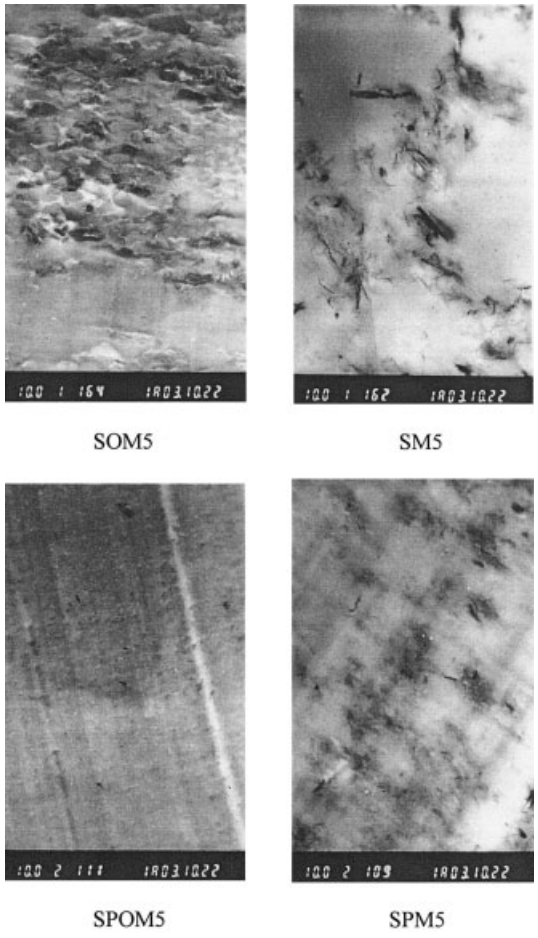

Figure 2 Transmission electron micrographs (TEM) of composites.

TABLE I
Polymer-Loading Content in Composites

Composites	Polymer-loading content (wt %)	Composites	Polymer-loading content (wt %)
SOM5	0.78	SM5	0.59
SPOM1	76.0	SPM1	70.6
SPOM2	65.2	SPM2	63.3
SPOM3	60.7	SPM3	58.8
SPOM5	57.2	SPM5	53.3
SPOM7	58.9	SPM7	52.8
SPOM10	56.9	SPM10	54.1

layer and the polymer matrix, which may act as compatibilizer. Compared with PS/clay composites, the clay dispersed in a high extent in St-PMI copolymer matrix, especially for SPOM5. It is apparent that the dispersability of OMMT and MMT in the St-PMI matrix is much better than that in the PS matrix.

Polymer-loading behavior

Table I compares the contents of polymer loading for the composites. The values of polymer content revealed by purified (after extraction) St-PMI/clay are much higher than that of PS/clay for both OMMT and MMT cases. This great difference in polymer loading is mainly a consequence of the incorporation of the PMI segment in the polymer backbone, which has higher interaction with clay.

Furthermore, the XRD patterns of the purified composites (demonstrated by adding a prefix "P-") are shown in Figure 3. The gallery distance of purified PS/clay nanocomposite is consistent with that of the clay before intercalation polymerization. This result also indicates the poor interaction of PS macromolecule with OMMT and MMT layers. For the case of purified St-PMI/clay composites, the XRD patterns show a large difference with different clay contents. The 001 *d*-spacing of the composites was changed with the change in clay content, but is much higher than that of the original clay, especially for St-PMI/OMMT composites, which is further evidence for the intercalation. The interlayer distances of composites are enlarged more than 1.26 nm for purified St-PMI/OMMT composites, which is much higher than 0.68 nm obtained from the melt intercalation of alkylammonium montmorillonite with PS.[5] Higher clay content, higher ordered layer structure, and smaller d_{001} were observed; even the layer structure could not be observed in the XRD pattern for P-SPOM2 composites.

It is worth noting that even for the St-PMI copolymer matrix, the gallery distance of the purified SP/

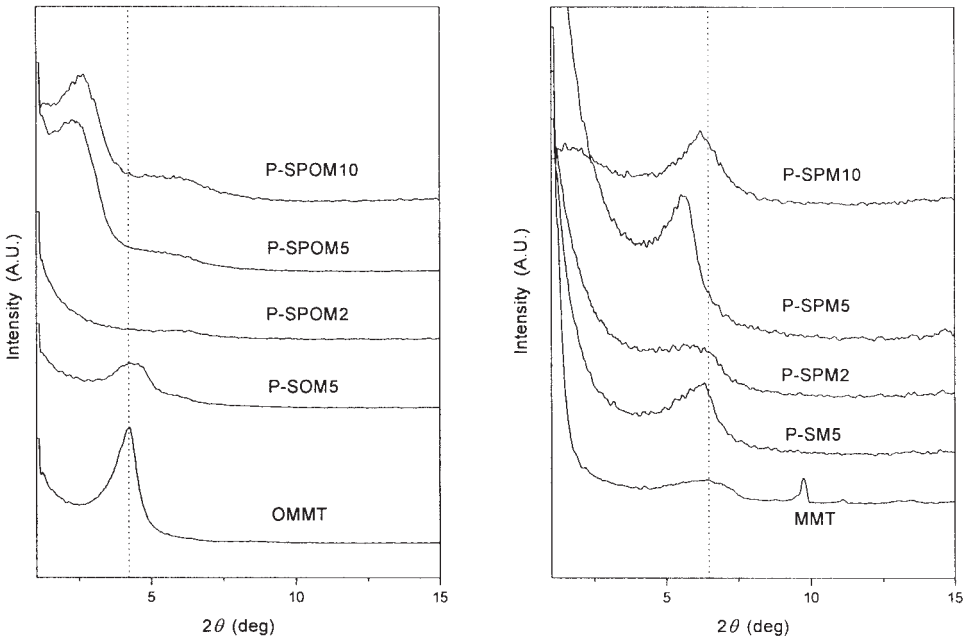

Figure 3 XRD patterns of extracted (purified) SPOM*x* and SPM*x* composites.

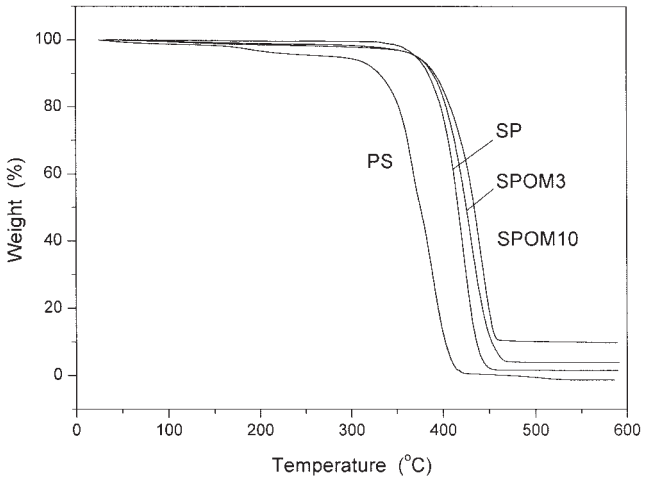

Figure 4 Thermograms of St-PMI/OMMT composites.

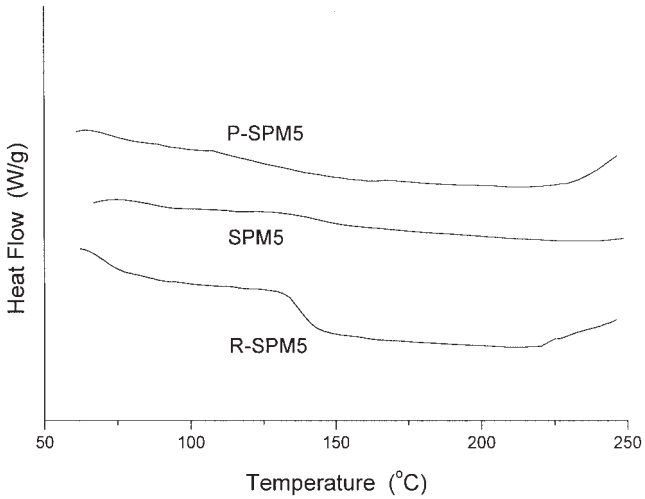

Figure 5 DSC curves of SPM5, P-SPM5, and recovered copolymer, R-SPM5.

OMMT composites is much higher than that of purified SP/MMT composites, which indicates that the copolymer chains are more liable to intercalate into the OMMT gallery than the MMT gallery.

Thermal characterization

Figure 4 shows TGA thermograms of weight loss as a function of temperature for PS, SP, and SP/clay composites. Evidently, the onset of thermal decomposition of SP/clay composites shifted significantly toward the higher temperature range than that of PS and SP, which confirms the enhancement of thermal stability of intercalated SP. The maximum weight loss rate temperatures, T_{max}, of the composites are summarized in Table II. T_{max} of the composites increased significantly with increasing clay content.

DSC traces of the recovered SP copolymer, composites, and purified composites are shown in Figure 5. The recovered polymer exhibits an endotherm at approximately 137°C, which is much higher than the 102°C of PS.[15] Nevertheless, the intercalated polymer does not show any traces of clear transitions. This is consistent with the results of PS/OMMT[5] and tentatively ascribed to the confinement of the intercalated polymer chains within the silicate galleries that prevents the segmental motions of the polymer chains.

TABLE II
T_{max} of St-PMI/OMMT and St-PMI/MMT Composites

Composites	T_{max} (°C)	Composites	T_{max} (°C)
PS	389.1	SP	422.4
SPOM1	424.8	SPM1	425.3
SPOM2	429.4	SPM2	428.0
SPOM3	431.6	SPM3	433.5
SPOM5	439.8	SPM5	436.0
SPOM7	440.7	SPM7	437.0
SPOM10	442.3	SPM10	437.3

Rheological properties

Figure 6 shows the apparent viscosities, η_a, versus shear rate for SP and SPMx at 200°C. η_a increased substantially at low shear rates. K (K is the consistency factor) and flow index n of the Ostwald–De Waele equation, $\eta_a = K\dot{\gamma}^{n-1}$, of the composites are calculated and shown in Figures 7 and 8. The inherent viscosities of the recovered copolymer are shown in Figure 9. Taking the influence of the molecular weight of the copolymer into account, K was found to increase monotonically with clay content. This may be caused by the frictional interactions between the anisotropic clay crystallites[18] because the flow activation energies of SPOM5 and SPM5 compounds (68.40 and 63.98

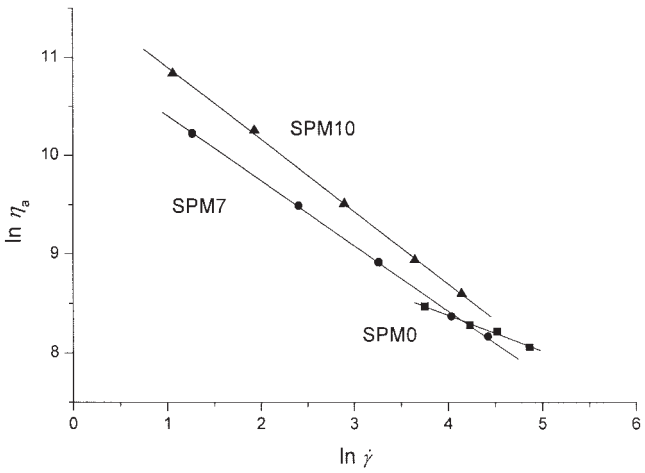

Figure 6 Apparent viscosities of melts of St-PMI/MMT.

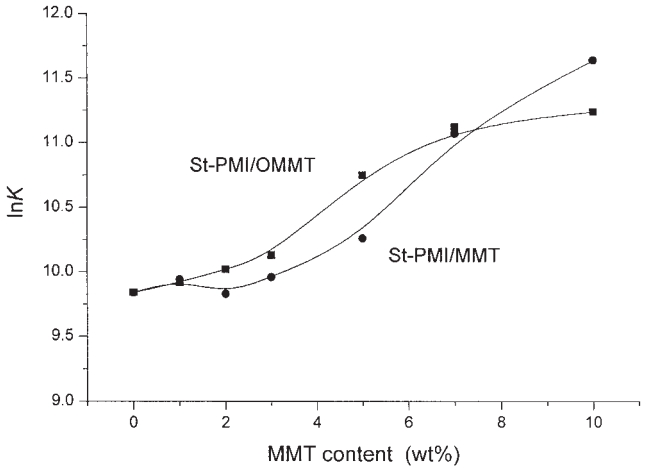

Figure 7 ln*K* of melts of St-PMI/OMMT and St-PMI/MMT composites.

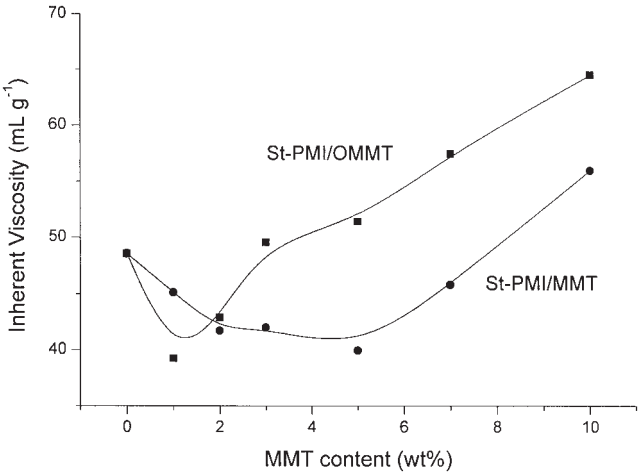

Figure 9 Inherent viscosities of recovered copolymer in St-PMI/OMMT and St-PMI/MMT composites.

kJ/mol) are even lower than that of the SP matrix (74.20 kJ/mol). At the same time, the composites exhibited stronger shear thinning than the copolymer since the chain entanglement and microstructure of the clay particles are transient. A similar trend was observed by Kim et al.,[9] Krishnamoorti et al.,[19] and others due to the changes in orientation of the silicate layers and polymer conformation under shear, as the silicate layers tend to be aligned by the application of shear flow.

CONCLUSIONS

St-PMI/clay composites could be prepared by emulsion polymerization of styrene and *N*-phenyl maleimide in the presence of montmorillonite. The interaction between the clay layer and the copolymer was greatly strengthened by the incorporation of PMI. Although the dispersability of OMMT in the matrix is much better than that of MMT, SP/MMT composites prepared with the pristine montmorillonite and a simple technique have nearly the same thermal, polymer-loading, and rheological properties as SP/OMMT composites.

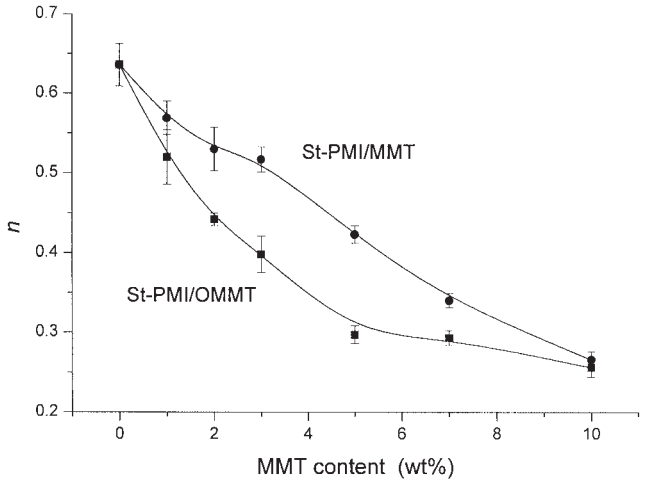

Figure 8 Flow indexes of melts of St-PMI/OMMT and St-PMI/MMT composites.

References

1. Okada, A.; Kawasumi, M.; Kurauchi, T.; Kamigaito, O. Polym Prepr 1987, 28, 447.
2. Pillion, J. E.; Thompson, M. E. Chem Mater 1991, 3, 777.
3. Yano, K.; Usuki, A.; Okada, A.; Kurauch, T.; Kamigato, O. J. Polym Sci Polym Chem 1993, 31, 2493.
4. Kojima, Y.; Usuki, A.; Kawasumi, M.; Okada, A.; Kutauchi, T.; Kamigato, O. J Polym Sci Polym Chem 1993, 31, 983.
5. Vaia, R. A.; Ishii, H.; Giannelis, E. P. Chem Mater 1993, 5, 1694.
6. Sikka, M.; Cerini, L. N.; Ghosh, S. S.; Winey, K. I. J Polym Sci Polym Phys 1996, 34, 1443.
7. Lee, D. C.; Jang, L. W. J. Appl Polym Sci 1996, 61, 1117.
8. Noh, M. H.; Jang, L. W.; Lee, D. C. J. Appl Polym Sci 1999, 74, 179.
9. Kim, T. H.; Jang, L. W.; Lee, D. C.; Choi, H. J.; Jhon, M. S. Macromol Rapid Commun 2002, 23, 191.
10. Laus, M.; Camerani, M.; Lelli, M.; Sparnacci, K.; Sandrolini, F. J. Mater Sci 1998, 33, 2883.
11. Okamoto, M.; Morita, S.; Kim, Y. H.; Kotaka, T.; Tateyama, H. Polymer 2001, 42, 1201.
12. Hasegawa, N.; Kawasumi, M.; Kato, M.; Usuki, A.; Okada, A. J. Appl Polym Sci 1998, 67, 87.
13. Kawasumi, M.; Hasegawa, N.; Kato, M.; Usuki, A.; Okada, A. Macromolecules 1997, 30, 6333.
14. Salahuddin, N.; Akelah, A. Polym Adv Technol 2002, 13, 339.
15. Liu, G.; Li, X.; Zhang, L.; Qu, X.; Liu, P.; Yang, L.; Gao, J. J. Appl Polym Sci 2002, 83, 417.
16. Liu, G. D.; Zhang, L. C.; Qu, X. W.; Wang, B. T.; Zhang, Y. J. Appl Polym Sci 2003, 90, 3690.
17. Zhang, Q.; Fu, Q.; Jiang, L.; Lei, Y. Polym Int 2000, 49, 1561.
18. Galgali, G.; Ramesh, C.; Lele, A. Macromolecules 2001, 34, 852.
19. Krishnamoorti, R.; Vaia, R. A.; Giannelis, E. P. Chem Mater 1996, 8, 1728.